Simulation of Tank sloshing in partially filled tanks using VOF[1] method

Hamid Rezaei, Mohammad Javad Ketabdari

Faculty of Marine Engineering
Amir Kabir University of Technology
HRezaei58@yahoo.com

Abstract

Sloshing in tanks carrying LNG, LPG and petroleum is an important phenomenon as dynamic pressure arises from sloshing can destroy the containing tanks. So it is vital to consider this phenomenon in design stages of carriers. The governing equations in fluid flow are conservation of mass and momentum. Modeling of free surface flow in tank needs a suitable tool. One of the most powerful tools to model the free surface is VOF method. Employing additional transport equation together with conservation of mass and momentum enable us to follow the free surface changes. A computer code was developed to evaluate sloshing problem. This code could calculate dynamic pressures exerted on walls of the containers. The model was validated using experimental data.

1. Introduction

From a structural point of view sloshing is critical in a partially filled tank. Dynamic pressure on the tank sides and bottom is increased due to sloshing. For accurate evaluation of this problem, we need a technique to compute the free surface profile. Between available techniques for computation of two phase flow such as MAC, VOF, LSM, VOF method was selected. In this paper a computer program based on VOF method was developed to calculate dynamic loads arise from sloshing in partially filled tanks. The results of the model were compared with experimental data.

2. Governing equations

2.1 Conservation Equations

The modeling of fluid flow can be described by mass and momentum conservation principles. It is assumed that fluid is incompressible and Newtonian. These are sufficient for the type of engineering applications considered here. Incompressibility implies that the density of the fluid is not dependent on the pressure, and for this type of fluid, the mass and momentum conservation can, in integral form, be written as:

$$\iint_\Gamma \vec{u}\cdot\vec{n}\,d\Gamma = 0 \tag{1}$$

$$\frac{\partial}{\partial t}\int_\Omega \vec{u}\,d\Omega = -\iint_\Gamma \left(\vec{u}\otimes\vec{u}\right)\cdot\vec{n}\,d\Gamma - \iint_\Gamma p\vec{n}\,d\Gamma + \frac{1}{Re}\iint_\Gamma \nabla\vec{u}\cdot\vec{n}\,d\Gamma \tag{2}$$

where $\vec{n}$ is the outward pointing normal vector at the boundary Γ of a volume element Ω, t is time, Re is the Reynolds number, $\vec{u}$ is the Cartesian velocity vector, and $\otimes$ is the outer vector product operator. Eqs. (1) and (2) are given for an Eulerian grid (e.g. fixed in time) but can be extended to arbitrary Eulerian-Lagrangian by inclusion of grid velocity in the convective term, which is the first on the right hand side of Eq. (2).

2.2. Spatial Discretisation

[1] Volume of Fluid

To solve the governing equations a domain is introduced in which the equations are solved. The discretisation scheme and the solution routine follow Zang et al. (1994). When the classic finite volume method is applied, the domain is discretised by subdivision into smaller non-overlapping control volumes, Ω_c, also denoted cells. Cartesian based structured grids are used in the present method, containing quadrilateral cells. A cell-centered variable arrangement is used for the discretisation scheme, and the governing equations are solved by use of the primitive variables of pressure and velocity. For a cell Ω_c with the cell boundary Γ_c the surface integrals can be discretised as a sum over the cell faces, Γ_f, and in discrete form the governing equations (Eq. (1) and Eq. (2)) can be rewritten as:

$$\sum_f \iint_{\Gamma_f} \vec{u} \cdot \vec{n}\, d\Gamma = 0 \tag{3}$$

$$\frac{\partial}{\partial t}\int_{\Omega_c} \vec{u}\, d\Omega = -\sum_f \iint_{\Gamma_f} \left(\vec{u} \otimes \vec{u}\right) \cdot \vec{n}\, d\Gamma - \sum_f \iint_{\Gamma_f} p\vec{n}\, d\Gamma + \frac{1}{Re}\sum_f \iint_{\Gamma_f} \nabla\vec{u} \cdot \vec{n}\, d\Gamma \tag{4}$$

where $\sum_f \Gamma_f = \Gamma_c$ and $\sum_c \Omega_c = \Omega$. Fig.1 illustrates the curvilinear discretised domain for a two-dimensional case.

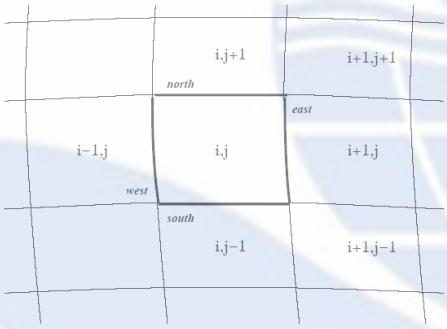

Figure 1: Cell layout for 2D structured grid. Cell Ω_c shown in bold.

3. Free Surface Modeling

The basis of the volume-of-fluid method is that to each cell an additional scalar is assigned which is the VOF (or volume fraction) value giving the degree of filling for the cell, Hirt, C. W. and Nichols, B.D., (1981). A cell with a volume fraction value of 0 is void, and a volume fraction value of 1 equals a full cell. If the value is between 0 and 1 the cell contains a free surface, i.e.:

$$\alpha = \frac{Volume\ of\ fluid\ in\ cell}{Total\ cell\ volume} \tag{5}$$

where α is the volume fraction and $1-\alpha$ is the volume fraction of the void or the air in the cell. Initially, all cells are given a volume fraction value, and at each time step a transport equation is solved to find the distribution of fluid at the new time step:

$$\frac{\partial \alpha}{\partial t} + \nabla \cdot \alpha\vec{u} = 0 \tag{6}$$

where t is time and $\vec{u}$ is the velocity vector.

The present study is based on a one-fluid approach, but the equations and derivations can easily be extended to a two-fluid approach. For a further description see Ubbink (1997). Moving grids can be applied in combination with the VOF method but are not used in this study.

4. Case Study

Sloshing problem experimentally conducted by Hinatsu et al. (2001). To validate the developed computer code, a tank with the same dimension of Hinatsu et al. (2001) experimental work was simulated. Fig.2 shows a schematic of setup in which the location of pressure gauges are indicated.

The computer code is not able to consider moving meshes. This requires that the coordinate system for which the computational domain inside the tank is defined has a moving frame of reference. This can be performed by adding a momentum source term to all computational cells. The magnitude of this source should be equal to acceleration of the frame of reference. The horizontal position of the tank is given by:

$$x = A\sin(\omega t) \tag{7}$$

where x is the horizontal position and ω is the angular frequency of the oscillation. The acceleration of the coordinate system, and hence the magnitude of the source can be found as:

$$\frac{\partial^2 x}{\partial t^2} = -A\omega^2 \sin(\omega t) \tag{8}$$

For all boundaries the wall boundary condition has been used with a viscosity equals to $10^{-6}\ \frac{m^2}{s}$. For all computations the maximum CFL number was selected as 0.2.

To investigate the grid sensitivity of the sloshing problem, three different network dimension meshes as: 96×48, 128×64 and 192×96 was used leading to cells with side length 12.5, 9.375 and 6.25 mm respectively. Fig.3 shows the pressure at gauges P1, P2 and P3 for different resolutions. The values of period and amplitude of the tank sloshing acceleration can be seen in Table 1, Case 1.

5. Visualization of the Fluid Motion

The experimental test with tank sloshing (Hinatsu et al., 2001) was performed in a rectangular tank with dimensions of 1200×600×200 mm. The tank was equipped with acrylic end plates in order to visualize the moving flow inside the tank. During the experimental tests the fluid motion inside the tank was captured using VCR. The tank was accelerated due to a horizontal sinusoidal motion. Pressure measurements were performed in the tank. Fig.2 shows the setup of the pressure gauges on the tank walls.

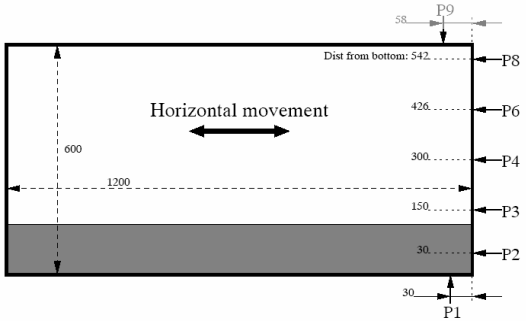

Figure 2: Sloshing tank setup (units [mm]). P indicates pressure gauge.

Table 1: Outline of sloshing cases.

	Water level	Period	Amplitude
Case 1	20 %	1.74 s	60 mm
Case 2	20 %	1.94 s	60 mm
Case 3	60 %	1.40 s	15 mm
Case 4	60 %	1.47 s	15 mm

Fig.4 presents single images of this visualization captured by video. This figure compares Case 1 at four different time steps for a 0.2 s time step between images. The first step (a) clearly shows a traveling wave inside the tank. The following pictures show the wave impact at the right side wall of the tank. A large amount of fluid separation at the free surface resulting from the wall impact is observed. The last images also show the formation of a new wave, which travels in the opposite direction. By comparison of experiments and computations the dynamics of the flow exhibits great resemblance. It can be seen that the traveling wave and the impact with the end wall are very similar to the experimental ones. However a large value of fluid separation observed in the experiments which is not captured in the computations. This could be arises due to following reasons: In one hand the developed code cannot resolve a fluid volume of smaller than a few grid cells. To capture very small amounts of fluid separation, a higher grid resolution is required. However, as this separation is not considered to be important for the overall flow dynamics, the effect of this phenomenon can be neglected. In the other hand, a part of separation is included as a result of three dimensional effects which cannot be captured with the two-dimensional numerical model.

Fig.5 presents a comparison of calculated pressure at gauges P1, P2 and P3 with measured pressure time series. For calculated pressure at Fig.5a to 8c the first two periods have been removed, as the fluid is not significantly excited yet. Furthermore the measurements were performed when the fluid was fully excited.

Fig.6 compares the values of gauges P1, P2 and P3 for Case 2. According to Hinatsu et al. (2001) this case is a no resonance case unlike the Case 1. This means that its fluid motion is less than that of Case 1. However Fig.6 shows that the magnitude of the measured pressure is very similar to that of Case 1. The comparison between measured and computed pressure is also similar to case 1, with the significant drop in pressure after each impact for both gauges P1 and P2. The last period in numerical results demonstrates better agreement with the experimental results than in Case 1 and the phase lag is not as evident.

6. Discussion and Conclusion

In general the numerical model performs very good predictions for the sloshing flow. The dynamics of the flow is well predicted as the visualizations show good agreement with numerical model for some distinct flow features, such as the traveling wave inside the tank and the impact at the end wall of the tank. The pressure levels inside the tank were also well predicted by the numerical model, since both the magnitude and the pressure time series for the impacts show good agreement. The 2-D modeling might over predict some flow features which do not occur in the experiments. The disagreement in the prediction of the accurate phase, where the computations showed a phase lag compared to the experiments, is more consistent. This starts after the first few periods, and grows throughout the simulation. The phase lag is due to loss of mass inside the domain. The magnitude of mass being removed is normally insignificant. However for applications such as the present sloshing case where a large amount of fluid separation from the free surface is involved, the amount of removed mass increases. This is significant to influence the flow properties, although the small region of separated fluid does not significantly influence the water flow in the domain. A new

scheme has been implemented in the code in order to avoid removing too large quantities of mass from the domain, but this was not completed at the time of the present simulations and will be a topic for further study.

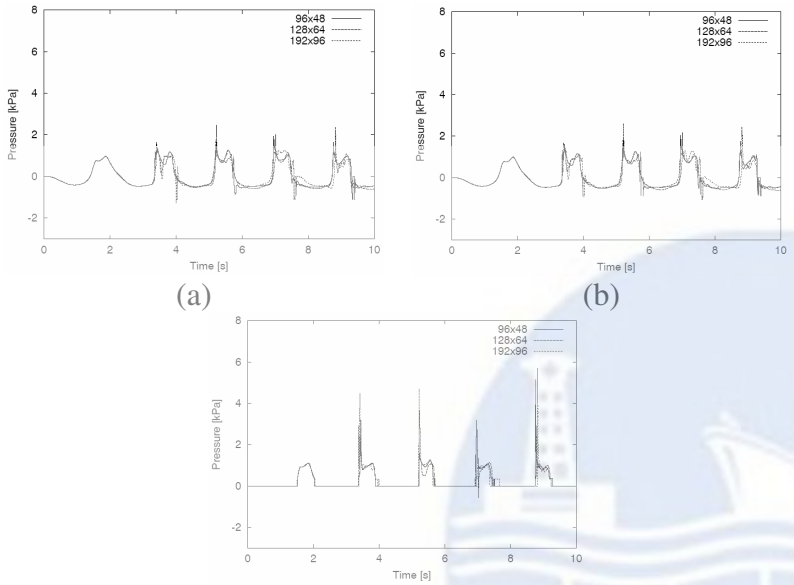

Figure 3: Computations of sloshing problem using three different grids (96×48, 128×64 and 192×96). The figures show the pressure computed inside the tank at P1 (a), P2 (b) and P3 (c).

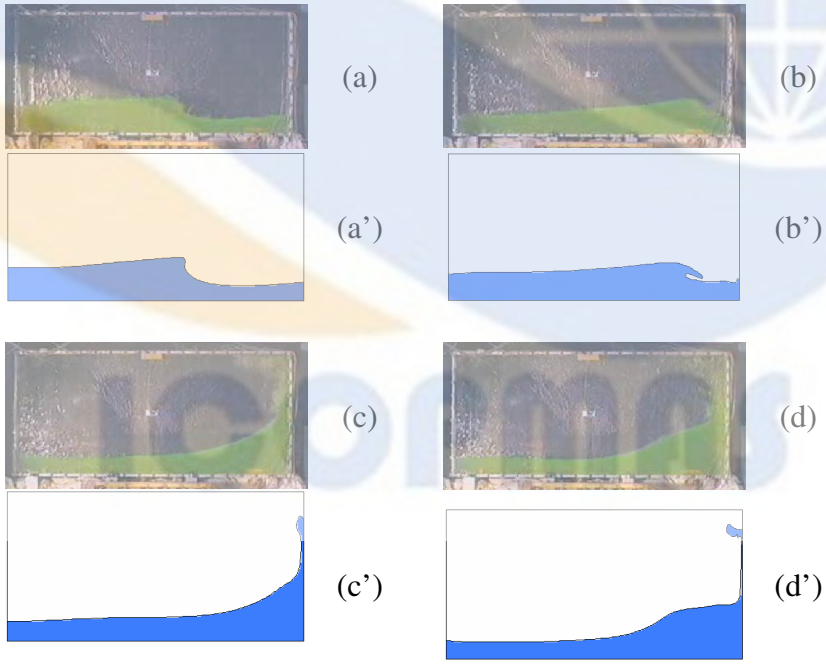

Figure 4: Visualization of the free surface contours in Case 1, for experiments and computations. Experiments are green and computations are blue.

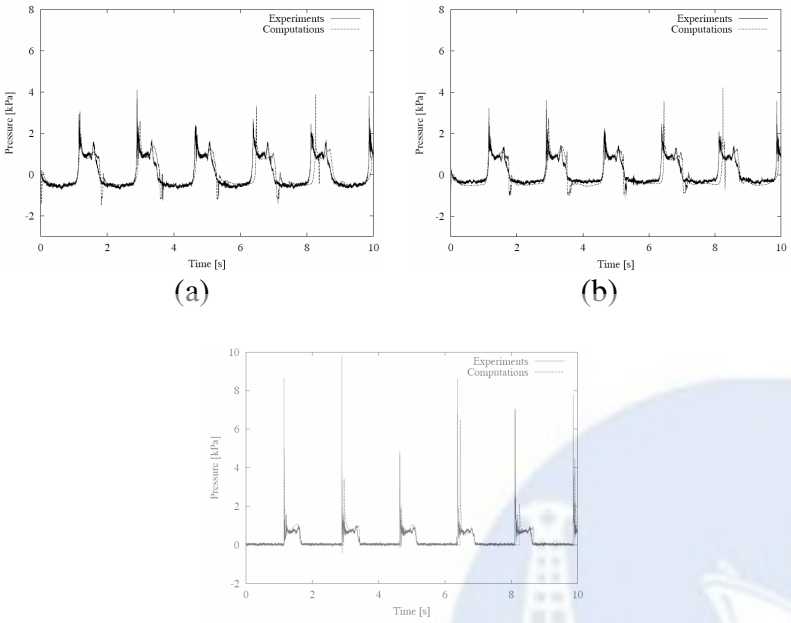

Figure 5: Comparison of numerical and experimental pressures, measured at gauges P1 (a), P2 (b) and P3 (c), for sloshing Case 1. The grid resolution equals 128×64 grid cells.

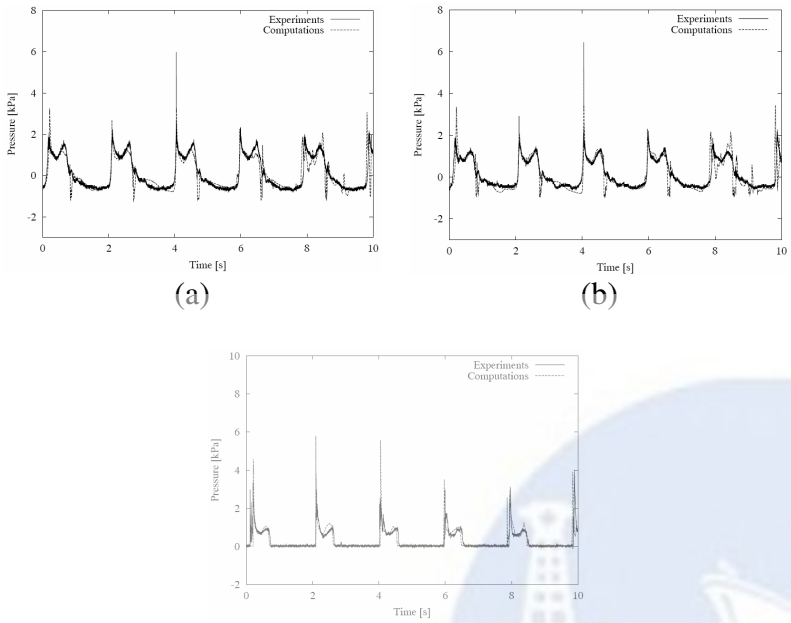

Figure 6: Comparison of numerical and experimental (Hinatsu et al., 2001) pressures, measured at gauges P1 (a), P2 (b) and P3 (c), for sloshing Case 2.

7. References

Hinatsu, M., Tsukada, Y., Fukusawa, R. and Tanaka, Y. (2001), Experiments of Two-Phase Flows for the Joint Research, *In Proceedings of SRI-TUHH mini-Workshop on Numerical Simulation of Two-Phase Flows*, edited by M. Hinatsu, pages 12–19. National Maritime Research Institute, Tokyo, Japan.

Hirt, C. W. and Nichols, B.D. (1981), Volume of fluid (VOF) method for the dynamics of free boundaries. *Journal of Computational Physics*, vol. 39: pages 201–225.

Ubbink, O. (1997), Numerical prediction of two fluid systems with sharp interfaces. *Ph.D. thesis*, University of London.

Zang, Y., Street, R. L. and Koseff, J. R. (1994), A non-staggered grid, fractional step method for the time incompressible Navier-Stokes equations in curvilinear coordinates. *Journal of Computational Physics*, vol. 114, pages 18–33.